Research Square

Preprints are preliminary reports that have not undergone peer review.
They should not be considered conclusive, used to inform clinical practice,
or referenced by the media as validated information.

Steady-state separability versus transition dynamics in single-channel sEMG during integrated upper-limb movement

Gabriela Lígia Reis
Federal Institute of Education, Science and Technology of Southeast Minas Gerais (IF Sudeste MG), Juiz de Fora
Márcio Falcão Santos Barroso
barroso@ufsj.edu.br
Federal University of São João del-Rei (UFSJ)
Eduardo Bento Pereira
Federal University of São João del-Rei (UFSJ)
Marcos Antônio Abdalla
SENAI Silvio Assunção Teixeira, FIEMG

Research Article

Keywords: surface electromyography, biomedical signal processing, myoelectric control, user-specific calibration, upper-limb movement, transition dynamics

Posted Date: September 10th, 2026

DOI: https://doi.org/10.21203/rs.3.rs-10744227/v1

License: This work is licensed under a Creative Commons Attribution 4.0 International License.
Read Full License

Additional Declarations: No competing interests reported.

Abstract

Purpose

To determine whether excellent steady-state separation of open and closed hand states is sufficient to characterize the dynamic performance of a single-channel surface electromyography (sEMG) interface during integrated upper-limb movement.

Methods

We performed a secondary analysis of an archived 2014 dataset from 20 adults without disabilities. Participants completed five hand-only trials and five integrated trials combining alternating hand opening/closing with proximal arm repositioning. We quantified participant-specific sEMG operating levels, steady-state separation using the area under the receiver operating characteristic curve (AUC), myoelectric transition midpoint (t50), functional output transition time, proximal-movement timing, and repetition effects.

Results

Established hand states remained almost completely separable in both conditions (mean AUC 0.997 hand-only vs 0.994 integrated; $p = 0.458$). In contrast, mean myoelectric t50 increased from 0.486 to 0.915 s (paired difference 0.430 s, 95% CI 0.262–0.597; $p < 0.001$; Cohen's $dz = 1.20$), with the largest protocol-specific penalty during closing transitions (0.521 to 1.367 s). A pooled retrospective decision boundary reproduced 80.6% of stored binary decisions, compared with 97.3% using participant-specific boundaries. Integrated-task t50 decreased from 1.141 to 0.820 s across repetitions (Friedman $p < 0.001$).

Conclusion

High steady-state separability does not imply fast dynamic performance. Evaluation of myoelectric interfaces should distinguish sustained-state discrimination from transition behaviour and should account for user-specific operating ranges, movement context, and state-dependent output logic.

Introduction

Surface electromyography (sEMG) is widely used in biomedical engineering to characterize muscle activation and to provide control information for human-machine interfaces. The surface recording, however, is not a direct readout of a single motor source: its amplitude and structure are influenced by neural drive, anatomy, volume conduction, electrode placement, contraction conditions, and movement (Farina et al. 2025; Reaz et al. 2006). Forearm sEMG has therefore been studied extensively for hand-

gesture recognition and robotic control, including investigations of feature processing, channel organization, and inter-individual factors (Tosin et al. 2020; Mendes Junior et al. 2020; Freitas et al. 2021).

A central engineering challenge is that performance measured from established labelled states may not represent performance while a user is changing state. Contemporary myoelectric systems can improve discrimination by using multiple channels, pattern-recognition methods, and richer sensing layouts (Simon et al. 2024), yet their robustness remains sensitive to limb position, electrode location, and task execution (Wang et al. 2024). High classification accuracy in static or segmented data can therefore coexist with limitations in real-time interaction.

Timing is particularly relevant in user-in-the-loop control. Offline classification metrics and online task performance can diverge (Campbell et al. 2025), undesired activations and response characteristics can affect functional myoelectric performance (Chadwell et al. 2021), and controller delay influences responsiveness (Farrell and Weir 2007). These findings suggest that sustained-state separability and transition dynamics should be treated as complementary performance dimensions rather than interchangeable measures.

User-specific calibration is another important component of minimally instrumented systems. During unsupported upper-limb activity, postural stabilization, co-contraction, proximal movement, and residual activation can modify a forearm recording even when the intended distal hand state is unchanged. Limb position can alter myoelectric features (Radmand et al. 2014; Wang et al. 2024), and a functionally open hand need not correspond to a zero-sEMG baseline. Consequently, the same absolute amplitude can have different functional meanings across users.

The dataset reanalysed here was acquired in 2014 during development of a multimodal upper-limb interface combining inertial sensing with single-channel sEMG (Reis 2014). Although the original electronics are not presented as a contemporary benchmark, the synchronized archive contains repeated myoelectric measurements, proximal kinematic context, stored output states, and repeated transitions. These data allow a technology-independent analysis of a question that remains relevant to biomedical signal processing: whether excellent discrimination of established states is sufficient to describe dynamic interface behaviour during concurrent movement.

The primary aim was therefore to determine whether high steady-state separability of single-channel sEMG is sufficient to characterize performance during an integrated upper-limb task. We examined (i) between-user variability and the rationale for individual calibration, (ii) the dissociation between sustained-state discrimination and transition timing, and (iii) the relation of transition dynamics to proximal-movement context and repeated interaction. We hypothesized that concurrent upper-limb activity would affect transition dynamics more strongly than the separability of already-established hand states.

Methods

Secondary reanalysis and recovered archive

This study is a secondary analysis of data originally collected in 2014 during the development and validation of a multimodal upper-limb human-machine interface (Reis 2014). No new participant data were collected. The recovered research archive included participant-specific raw and processed sEMG files, effector-state records, inertial/reference trajectories, five repetitions of the experimental conditions, LabVIEW virtual instruments, MATLAB analysis scripts, and the original dissertation documentation.

The present analysis was designed after recovery of these source files and addresses outcomes that were not the focus of the original work. Participant identities were replaced by codes P01-P20 for the reanalysis. Original files were retained unchanged; derived files and analyses were created separately.

Participants and experimental platform

The original experiment included 20 adults without disabilities, of both sexes, aged 19–40 years (Reis 2014). The experimental platform combined a forearm-mounted inertial measurement system, a single-channel surface electromyograph, a computer running LabVIEW, and a LEGO Mindstorms robotic manipulator. The robot had two proximal joint motions corresponding to yaw and pitch and an effector that opened and closed. Its role was to provide an observable physical representation of the inferred arm and hand action; it was a rapid-prototyping and feedback platform rather than the intended final target device (Reis 2014).

Figure 1 shows the components most relevant to the present reanalysis. The inertial module was mounted on the distal forearm to estimate proximal orientation. Bipolar surface electrodes recorded forearm sEMG, with a separate reference electrode. The robotic manipulator reproduced the inferred yaw, pitch, and effector state so that the participant could observe the consequence of the interface output. This arrangement links the physiological signal, kinematic context, and functional output that are analysed below.

The proximal yaw and pitch loops used a conventional fuzzy controller, whereas the hand effector used binary on-off logic. Because these controllers acted on different variables and served different functions, they are not treated as competing controller architectures. Representative platform-level validation traces are shown in Fig. 5. In the original validation, robot angular position followed the inertial-system reference trajectories with low settling time, no sustained oscillation around the commanded positions, and a reported angular tracking error below 1 degree (Reis 2014). This evidence is used only to establish that the robotic platform provided responsive kinematic feedback; controller comparison is not an outcome of the present secondary analysis.

Hand-only and integrated upper-limb protocols

In the hand-only condition, a graphical interface instructed participants to alternate between open and closed hand states. Each participant completed five 60-s trials, with the requested state changing approximately every 10 s. The arm was not required to follow the sequence of proximal configurations used in the integrated condition.

In the integrated condition, the same alternating hand requirement was embedded within a sequence of proximal arm configurations. Five 60-s trials were completed. Figure 2 reconstructs the six successive configurations from the original photographs and archived reference trajectories. The sequence was P1 (yaw 0 degrees, pitch 0 degrees, hand closed), P2 (0 degrees, + 45 degrees, hand open), P3 (+ 90 degrees, 0 degrees, hand closed), P4 (0 degrees, -45 degrees, hand open), P5 (-90 degrees, 0 degrees, hand closed), and P6 (0 degrees, 0 degrees, hand open). The five state changes are labelled T1-T5 throughout the Results: T1, T3, and T5 are opening transitions; T2 and T4 are closing transitions.

The integrated protocol is important for interpretation because a single forearm recording was obtained while the participant simultaneously repositioned and stabilized an unsupported upper limb. Proximal movement, postural stabilization, co-contraction, and the distal hand action could therefore all influence the measured physiological activity. The experiment did not record individual muscle sources, so the present study does not attempt to assign the observed sEMG changes to specific muscles.

sEMG acquisition and user-specific calibration

Hand-state inference used a one-channel surface electromyograph developed for the original system. The analogue signal was amplified, filtered, rectified, and digitized (Reis 2014). The nominal sEMG sampling frequency was 1000 Hz. In the online application, mean signal amplitude was calculated over 240-sample windows, corresponding to a nominal decision update every 0.24 s.

At the start of each complete experimental session, before the set of five trials, the original protocol used an individual calibration procedure. The dissertation describes the decision reference as being established from the maximum mean sEMG observed with the hand open (Reis 2014). The calibrated decision boundary was then retained throughout the five repetitions in that session; participants were not recalibrated between repetitions. This approach is functionally important because an open hand during an unsupported arm task can retain a positive sEMG baseline; the classification boundary was therefore user-specific rather than referenced to zero.

The exact online calibration value was not stored for every trial in the recovered archive. We therefore reconstructed an effective decision boundary from the persisted hand-only data. Persisted sEMG samples were grouped according to their associated effector/control record (typically 200 stored values per record), and the block mean was compared with the stored binary decision. For each participant or repetition, a scalar boundary was selected retrospectively to maximize agreement with the original stored decisions. These values are termed reconstructed effective persisted-data boundaries. They are

not assumed to be statistically identical to, or exact recoveries of, the original 240-sample online calibration constants.

One hand-only record (P06, repetition 1) contained an apparent concatenation anomaly and was excluded from boundary reconstruction. After this exclusion, 25,067 persisted control blocks were available. Agreement obtained by fitting boundaries to these same archived blocks is reported only as a descriptive replay of the stored decision logic, not as cross-validated predictive accuracy.

Context-aware state logic

The original hand controller used binary on-off logic with effector-state memory: an opening or closing actuation was required only when the inferred hand state differed from the current effector state (Reis 2014). In the complete LabVIEW implementation, sensing, proximal-joint control, and effector actions were coordinated within a state-based program structure.

For the present engineering interpretation, the measured sEMG is treated as physiological evidence rather than as a self-sufficient actuator command. Individual calibration defined how signal amplitude was interpreted for a given participant, inertial sensing provided proximal-movement context, and the current system state constrained whether a new effector action was required. This combination is referred to here as context-aware state logic. It does not imply physiological source decomposition of the single-channel sEMG.

This architectural description is used to clarify the operating principle of the original interface. The present secondary analysis does not experimentally compare context-aware logic with an alternative controller architecture.

Temporal reconstruction and outcome measures

The recovered archive contains different temporal resolutions for internal acquisition and persisted logging. Although online sEMG processing nominally used 240 samples at 1000 Hz, persisted files typically contained 200 sEMG values for each recorded effector/control update. The median interval between successive persisted control records was approximately 0.23 s. Accordingly, the present timing outcomes are functional transition measures at the resolution of the stored control sequence; they should not be interpreted as high-resolution electrophysiological onset times or reported with millisecond precision.

Four complementary outcome domains were analysed. First, stable open- and closed-hand operating levels and reconstructed effective boundaries were used to describe between-user amplitude variability. Second, sustained-state discrimination was quantified with the area under the receiver-operating-characteristic curve (AUC) after excluding the first 3 s following each requested transition. AUC was calculated directly from labelled stable-state amplitudes; it did not use the reconstructed threshold and was not a trained classifier performance estimate.

Third, myoelectric transition shape was quantified after normalizing each trial so that its stable open-hand level represented 0 and its stable closed-hand level represented 1. For each requested change, we identified the first 20%, 50%, and 80% crossing toward the new state that persisted through the next stored control record. The 50% measure (t50) is used as the primary myoelectric transition time. The 20% and 80% points describe whether a delay arose before the middle of the transition or during the subsequent progression. These are operational markers of the archived signal, not physiological motor-unit onset thresholds.

Fourth, functional output transition time was defined from the requested hand-state change to the first correct output state that remained correct through the next stored record. In the integrated protocol, proximal movement onset was operationally defined as the time at which combined angular displacement exceeded 5 degrees. Sensitivity checks using 3-, 7-, and 10-degree criteria preserved the qualitative event ordering. For event-centred protocol tracking, each requested transition was used as the common time-zero anchor, allowing proximal-movement onset, myoelectric transition markers, and functional output timing to be compared on the same temporal reference.

Statistical analysis

Participant was treated as the principal inferential unit whenever repeated windows or events could otherwise produce pseudoreplication. Hand-only and integrated conditions were compared using paired Student's t-tests, with Wilcoxon signed-rank tests used as non-parametric sensitivity analyses. Mean paired differences are reported with 95% confidence intervals. Cohen's dz was used for within-participant effect size where reported.

Repeated-trial effects were assessed with the Friedman test and a paired comparison between repetitions 1 and 5. Event-specific associations between proximal movement onset and myoelectric transition time were first examined from participant-level event means using Pearson correlation. An exploratory repeated-observation linear model accounting for participant, repetition, and event was used to examine whether movement timing remained associated with myoelectric transition time. All tests were two-sided with alpha = 0.05. Because the analyses are secondary and hypothesis-generating, exact p-values and effect sizes are emphasized over dichotomous significance labels where practical.

Ethical considerations

The source data were collected in 2014 in a non-invasive engineering validation involving adult university volunteers without disabilities. The protocol comprised voluntary upper-limb movement, surface electromyography, inertial sensing, and visual robotic feedback; it did not include diagnosis, treatment, medication, invasive procedures, or electrical stimulation. Formal research-ethics committee review was not sought at the time. Participation was voluntary after verbal explanation of the experimental procedure, and written informed consent was not obtained. The present study is a secondary analysis of de-identified archived data; no new participants were recruited and no new intervention or data collection was performed.

AI-assisted manuscript preparation

OpenAI ChatGPT (GPT-5.6 Sol) was used during preparation of the present manuscript as an assistive tool for manuscript organization, language editing, code drafting supporting the secondary reanalysis, literature-search support, and preparation of non-generative data visualizations. No generative AI was used to create, alter, or synthesize research data or participant images. All numerical results, references, interpretations, code outputs, and final text were reviewed by the authors, who take full responsibility for the integrity and accuracy of the manuscript.

Results

Inter-user variability and the need for calibration

The most important feature of the participant-level sEMG data was not the absolute voltage but the shift of the operating range from one user to another. Across participants, the median stable open-hand level ranged from 0.038 to 0.245 V, while the median stable closed-hand level ranged from 0.090 to 0.388 V. Median reconstructed effective boundaries ranged from 0.052 to 0.299 V (Fig. 3). Thus, a positive sEMG level did not have a universal functional meaning.

The between-user overlap was substantial. In 55 of 380 directed pairwise comparisons (14.5%), the median open-hand level of one participant exceeded the median closed-hand level of another. P20 provides the clearest visual example: this participant's median open-hand level (0.245 V) was higher than the closed-hand median of 16 of the other 19 participants. This pattern does not indicate poor discrimination within P20; it shows why a fixed amplitude boundary transferred between people can be inappropriate.

The reconstructed boundaries produced the same message when used as a descriptive replay of the archived decisions. A single pooled boundary fitted to all 25,067 valid stored blocks reproduced 80.6% of the original binary decisions. A single participant-specific boundary, fitted across that participant's repetitions, increased agreement to 97.3%. Repetition-specific fits reproduced 99.98% of stored decisions, confirming that a scalar amplitude boundary closely described the archived binary logic within a repetition. Because these boundaries were fitted retrospectively to the same records on which replay agreement was assessed, the percentages are not estimates of prospective classification accuracy.

Dissociation between stable performance and transition dynamics

The original analysis reported very high overall hand-state accuracy in both protocols. Mean participant accuracy decreased from 99.16% in the hand-only condition to 98.37% in the integrated condition, a paired change of -0.79 percentage points (95% CI -1.44 to -0.14; paired t $p = 0.019$; Wilcoxon $p = 0.0066$).

If evaluation stopped at this aggregate accuracy measure, the integrated task would appear to produce only a small performance reduction.

The reanalysis separates two different questions: whether open and closed states can be distinguished after they have stabilized, and how long the user-interface system takes to establish the new state. Once stable, the two states remained almost completely separable. Mean AUC was 0.997 in the hand-only condition and 0.994 in the integrated condition, with no evidence of a paired difference ($p = 0.458$; Fig. 4A). In practical terms, concurrent arm movement did not collapse the distinction between established open and closed sEMG states.

Transition behaviour changed much more strongly. Mean myoelectric t50 increased from 0.486 s in hand-only trials to 0.915 s in integrated trials, a paired increase of 0.430 s (95% CI 0.262–0.597; $p < 0.001$; $dz = 1.20$; Fig. 4B). The corresponding functional output transition time increased from 0.529 to 0.929 s (paired increase 0.399 s, 95% CI 0.254–0.545; $p < 0.001$). The mean difference between myoelectric and output transition time in the integrated condition was approximately 0.013 s, smaller than the effective temporal resolution of the stored data; therefore, the archive provides no evidence that the large integrated-task penalty was introduced primarily after the myoelectric state had become established.

Table 1 condenses these three complementary findings for an interdisciplinary reader. AUC near 1 means that sustained open and closed states are almost completely distinguishable; the transition-time rows quantify the additional time needed to establish the new physiological and functional states. The central dissociation is therefore preserved steady-state discrimination alongside substantially slower transitions.

Table 1
Main findings: sustained-state discrimination versus transition performance.

Outcome	Hand-only	Integrated	Paired change (95% CI; p)	Functional interpretation
Stable hand-state discrimination (AUC; 1.0 = complete separation)	0.997	0.994	-0.003 (-0.011 to 0.005); p = 0.458	Established open and closed states remained almost completely distinguishable.
Myoelectric transition time, t50 (s)	0.486	0.915	+ 0.430 (+ 0.262 to + 0.597); p < 0.001	The physiological hand state took longer to become established during the integrated task.
Functional output transition time (s)	0.529	0.929	+ 0.399 (+ 0.254 to + 0.545); p < 0.001	A comparable transition delay was observable at the interface output.

Direction-specific analysis provides additional description but must be interpreted within the fixed sequence of Fig. 2. For opening transitions, mean myoelectric t50 increased from 0.462 to 0.614 s (difference 0.152 s; $p = 0.031$). For closing transitions, it increased from 0.521 to 1.367 s (difference 0.847 s; $p < 0.001$; dz approximately 1.30). Because opening/closing direction is coupled to event position and proximal configuration, this asymmetry should be treated as protocol-specific rather than as proof of a general physiological difference between opening and closing.

Transition-shape analysis showed that the closing penalty began before the signal reached the middle of the new operating range. For closing transitions, mean t20 increased from 0.372 to 1.016 s and t80 from 0.642 to 1.557 s; the 20–80% progression itself lengthened from 0.270 to 0.540 s. Across all transitions, t20 increased by 0.299 s, t50 by 0.430 s, and t80 by 0.478 s. This pattern is more consistent with delayed departure from the previous operating state plus slower progression toward the new state than with simple threshold chatter after the decision boundary had already been reached.

Platform tracking, task context, and repetition effects

Before interpreting the within-transition delays, it is useful to separate the timing of the robotic feedback layer from the timing of the user-interface state transition. The original platform-validation tests used step-like yaw and pitch trajectories over 60 s and showed close tracking of the inertial-system references by the robot (Fig. 5). These traces are not the participant-level trials used for the t50 analysis; they are included as platform validation so that the dynamic results below are not mistaken for a gross failure of proximal robotic tracking.

Figures 5 and 6 separate two timing questions that would otherwise be easy to conflate. Figure 5 concerns platform tracking on the 60-s sequence scale. Figure 6 concerns the first approximately 1.5 s after each requested hand-state change in the integrated trials. For Fig. 6, each request is defined as $t = 0$; the 5-degree criterion marks the onset of meaningful proximal displacement, and t50 marks the point at which the normalized sEMG reached the midpoint of the new hand state. In the integrated condition, functional output followed the myoelectric t50 by only approximately 0.013 s on average, which is smaller than the effective temporal resolution of the archived control log. Thus, the large condition-related delay identified here occurs before or while the new myoelectric state is being established rather than being introduced mainly after state detection by the robot/output-control stage.

On this common event-centred time base, mean myoelectric t50 was 0.587, 1.373, 0.635, 1.362, and 0.620 s for T1-T5, respectively, while mean proximal 5-degree movement onset occurred at 0.912, 0.856, 0.755, 0.780, and 0.922 s. The five transitions did not support a simple interpretation that greater proximal movement necessarily produced a slower myoelectric hand transition. T3 is particularly informative: it had the largest mean angular displacement during the first second (39.4 degrees) and the highest mean speed (41.1 degrees/s), yet its myoelectric transition remained relatively fast at 0.635 s (Fig. 6). Movement magnitude alone therefore does not explain the delay.

Temporal ordering was more informative. During the three opening events, the myoelectric midpoint generally occurred before the 5-degree proximal-movement criterion. During the two closing events, proximal movement was already underway before the myoelectric closing state reached its midpoint. Across participants, later proximal movement onset was positively associated with longer myoelectric transition time in every event (Pearson r = 0.54–0.77). In an exploratory repeated-observation model accounting for participant, repetition, and event, a 1-s later proximal onset was associated with approximately 0.66 s additional myoelectric transition time (95% CI 0.44–0.88; $p < 0.001$). When movement speed was added to the same model, the onset term remained informative whereas speed did not, supporting an interpretation centred on temporal organization rather than movement magnitude alone.

Repeated interaction changed the integrated-task transition. Mean myoelectric t50 decreased from 1.141 s in repetition 1 to 0.974, 0.801, 0.841, and 0.820 s in repetitions 2–5 (Friedman $p < 0.001$; Fig. 7). The paired repetition-1 to repetition-5 reduction was 0.321 s (95% CI 0.093–0.548; $p = 0.008$). Because the same calibration boundary was retained throughout the five repetitions of a session, this improvement cannot be attributed to recalibration between trials. The study did not include an objective fatigue measure or standardized subjective workload assessment, so fatigue cannot be excluded as a contributor to individual trials. However, the group-level reduction in transition time over repetitions does not support cumulative fatigue as the dominant explanation for the observed pattern.

Functionally, the repetition result is distinct from calibration. Calibration identified where an individual's open and closed operating ranges lay at the start of the session, whereas the same boundary was then held constant across the five trials. The progressive change in transition timing therefore reflects a change in the person-interface task rather than a trial-by-trial change in the decision boundary. This distinction is relevant to interface evaluation because static state production and transitions during concurrent movement may represent different aspects of user-interface skill.

Discussion

Principal findings

This secondary analysis changes the interpretation of an experiment that originally appeared to be dominated by very high classification percentages. Three findings are central. First, absolute single-channel sEMG operating levels varied substantially between users, so a voltage compatible with an open hand in one participant could exceed the closed-hand level of another. Second, stable open and closed states remained almost completely separable in both hand-only and integrated conditions. Third, transition behaviour changed markedly: mean myoelectric t50 almost doubled during the integrated task, and the largest protocol-specific penalty occurred during closing transitions.

Together, these findings demonstrate a dissociation between steady-state discrimination and dynamic performance. The original aggregate accuracy changed by less than one percentage point, whereas

myoelectric transition time increased by approximately 0.43 s. The output state then followed the myoelectric midpoint with no resolvable additional delay in the archived integrated logs. Accordingly, a system can classify established states extremely well while still requiring substantially more time to establish a new physiological state during concurrent movement. For biomedical interface evaluation, accuracy or AUC alone can therefore miss a performance limitation that becomes visible only when the temporal sequence from request to movement, myoelectric state establishment, and output is analysed explicitly.

Context-dependent interpretation of single-channel sEMG

Single-channel sEMG cannot identify all muscle sources contributing to a forearm surface recording, particularly during an unsupported multi-joint task (Farina et al. 2025). The present results do not imply that proximal activity is spurious EMG. Stabilizing and repositioning the arm can produce physiologically appropriate activation; the engineering problem arises when biologically valid activity is interpreted as though it necessarily represented a new distal hand command.

The original architecture addressed this ambiguity pragmatically rather than through physiological source separation. Individual calibration assigned participant-specific meaning to amplitude, inertial sensing described proximal motion, and state-based logic constrained whether the current estimate required a new output action. In this sense, sensor signals provide evidence, whereas calibration, context, and system state constrain how that evidence is translated into device behaviour.

This principle complements rather than competes with richer sensing and signal-processing approaches. Multi-channel sEMG can provide additional spatial information, and forearm sEMG studies have demonstrated the value of multichannel processing and subject-related analysis for hand-gesture recognition (Freitas et al. 2021; Mendes Junior et al. 2020). At the same time, contemporary studies continue to report sensitivity to limb position and electrode shift (Wang et al. 2024) and divergence between offline classification and online user performance (Campbell et al. 2025). Context-dependent interpretation is therefore relevant even when hardware and classifiers are more sophisticated than those used in the original experiment.

Relation to contemporary myoelectric signal processing

The historical hardware is a limitation for claims about contemporary electronics, sampling architecture, or embedded implementation. It is not used here as a benchmark. The value of the archive lies instead in its synchronized combination of sEMG, proximal kinematics, output state, and repeated requested transitions, which makes it possible to compare stable-state separability with dynamic transition behaviour within the same participants. The original platform-validation traces document responsive proximal robot-to-inertial-reference tracking (Fig. 5), but they are not the same participant trials used for the transition analysis. More directly, the integrated logs show that functional output followed myoelectric t50 by only approximately 0.013 s, below the effective logging resolution. Read together with the event-centred organization in Fig. 6, these observations argue against interpreting the main transition penalty as a delay introduced predominantly after the myoelectric state had already been established.

The underlying engineering problem remains current. Recent work shows that channel configuration can affect online completion time and path efficiency (Simon et al. 2024), limb position and electrode displacement alter myoelectric feature spaces (Wang et al. 2024), and models with lower offline accuracy can outperform higher-accuracy alternatives during user-in-the-loop interaction (Campbell et al. 2025). Studies focused on responsiveness likewise continue to treat timing as an explicit control variable (Won and Iwase 2025). The present dataset contributes a complementary observation: dynamic degradation can occur even when steady-state class separability remains nearly unchanged.

The original sensing concept was subsequently extended by the group toward wireless inertial sensing and sensor-fusion implementations (Santos et al. 2019; Santos et al. 2020). Those later developments are not outcomes of the present study, but they reinforce the distinction between the historical prototype and the technology-independent question examined here.

Engineering implications for myoelectric interface evaluation

The first implication is methodological: sustained-state classification and transition performance should be reported separately when a myoelectric interface is intended to operate during ongoing movement. In this dataset, AUC remained near 1.0 while t50 increased substantially. Evaluating only prolonged static postures would therefore have produced an incomplete description of interface behaviour.

The second implication concerns calibration. A universal absolute amplitude boundary assigned inconsistent meanings across participants, whereas participant-specific boundaries reproduced the archived binary decisions much more closely. This result supports individualized operating ranges whenever a low-channel-count interface relies strongly on amplitude information. Calibration answers where a user's functional states lie in the measurement space; transition analysis answers how rapidly the user-interface system moves between those states under the current task context.

The third implication concerns repeated interaction. Transition time decreased across the five integrated repetitions while the same calibration boundary was retained. The pattern is consistent with short-term familiarization or adaptation of the person-interface task rather than with recalibration. Although the experiment was not designed as a training study, the result indicates that repeated-trial effects should be considered when evaluating dynamic myoelectric performance (Heerschop et al. 2024; Mamidanna et al. 2024; Wu et al. 2021).

Finally, state-dependent output logic should be viewed as an architectural means of preventing every physiologically valid fluctuation from becoming a new device command, not as evidence of proven safety or superior control. The present study did not compare controller architectures. Future work should test whether combining individualized calibration, movement context, and explicit state logic improves online performance relative to alternative low-channel-count strategies.

Limitations

The dataset was acquired in 2014 from adults without disabilities. The results therefore describe engineering behaviour in the tested experimental context and cannot be interpreted as direct performance estimates for people with amputation, neurological impairment, or other motor disabilities. Testing in target user populations remains necessary before generalizing the findings beyond the population and task studied here (Reis 2014).

Only one sEMG channel was recorded. The study cannot identify individual muscle contributions or distinguish the relative roles of co-contraction, cross-talk, postural stabilization, attention, motor planning, or other physiological mechanisms. Context-dependent interpretation therefore refers to the functional decision level, not to physiological source decomposition.

The integrated sequence was fixed. Hand direction was coupled to event position and proximal configuration; consequently, the larger closing-transition penalty cannot be generalized as an intrinsic physiological difference between closing and opening. A randomized or counterbalanced protocol would be required for that conclusion.

Persisted logging had lower effective temporal resolution than the nominal 1000-Hz acquisition. The reported transition times are functional measures at approximately 0.23-s control-record resolution, not precise neuromuscular onset latencies. The exact online calibration threshold was not retained for every trial; reconstructed effective boundaries reproduce the persisted decision behaviour but are not the original calibration constants.

Fatigue, perceived effort, workload, satisfaction, naturalness, and other subjective user-experience outcomes were not systematically measured. The study therefore cannot establish how the approximately 0.9-s integrated transition was perceived by participants or define a user-acceptable or application-specific delay. It should also not be directly compared with studies that experimentally add controller delay, because the present measure includes the time required for the user's physiological state itself to become established.

Conclusion

In this archived multimodal upper-limb dataset, concurrent proximal movement had little effect on the separability of already-established open and closed hand states but substantially increased the time required for the myoelectric state to become established. The central finding is therefore a dissociation between excellent steady-state discrimination and slower transition dynamics.

The results also demonstrate the importance of interpreting absolute single-channel sEMG amplitude relative to the individual. Between-user operating ranges overlapped strongly, whereas within-user separation remained useful. User-specific calibration, kinematic context, and state-dependent output logic can therefore be viewed as complementary mechanisms for qualifying physiological information in minimally instrumented myoelectric interfaces.

For biomedical engineering evaluation, high steady-state accuracy should not be treated as sufficient evidence of responsive dynamic interaction. Transition timing, task context, and repeated-interaction effects provide additional information that can reveal limitations concealed by static classification metrics.

Declarations

Ethics approval:

The source data were collected in 2014 in a non-invasive engineering validation involving adult university volunteers without disabilities. The procedure comprised voluntary upper-limb movement, surface electromyography, inertial sensing, and visual robotic feedback; it did not involve diagnosis, treatment, medication, invasive procedures, or electrical stimulation. Formal research-ethics committee review was not sought at the time. The present study is a secondary analysis of de-identified archived data, with no new participant recruitment, intervention, or data collection.

Consent to participate:

Participation in the 2014 engineering validation was voluntary after verbal explanation of the experimental procedure. Written informed consent was not obtained.

Consent to publish:

No identifiable participant information is presented. Historical photographs were cropped to exclude faces and direct personal identifiers.

Competing interests:

The authors declare no competing interests.

Funding:

The original research environment received support from Fundação de Amparo à Pesquisa do Estado de Minas Gerais (FAPEMIG), Coordenação de Aperfeiçoamento de Pessoal de Nível Superior (CAPES), and Conselho Nacional de Desenvolvimento Científico e Tecnológico (CNPq), including support for scholarships, research infrastructure, equipment, travel, and scientific dissemination. No specific grant is attributed to the present secondary analysis, and no additional funding was received for preparation of this manuscript.

Author Contribution

Gabriela Lígia Reis: Investigation, Software, Data Curation, Validation, Methodology, and Writing – Original Draft. Márcio Falcão Santos Barroso: Conceptualization, Methodology, Supervision, Project Administration, Formal Analysis, and Writing – Review & Editing. Eduardo Bento Pereira: Supervision, Methodology, Validation, and Writing – Review & Editing. Marco Antônio Abdalla Junior: Methodology, Instrumentation, Validation, and Writing – Review & Editing. All authors reviewed and approved the final version of the manuscript.

Acknowledgement

The authors gratefully acknowledge the support of the Fundação de Amparo à Pesquisa do Estado de Minas Gerais (FAPEMIG), the Conselho Nacional de Desenvolvimento Científico e Tecnológico (CNPq), and the Coordenação de Aperfeiçoamento de Pessoal de Nível Superior (CAPES). The authors also acknowledge the Graduate Program in Electrical Engineering (PPGEL) and the institutional research environment provided by the Federal University of São João del-Rei (UFSJ), particularly the Center for Robotics and Assistive Technologies (CyRoS), as well as the students and researchers who contributed to the original experimental activities.

Data Availability

The participant-level dataset analysed during the current study is not publicly available because the original 2014 consent process did not include provisions for public data sharing. De-identified derived data and analysis code may be made available by the corresponding author upon reasonable request, subject to institutional and ethical considerations. No new participant data were collected for the present study.

Code availability:

Analysis code supporting the secondary reanalysis may be made available by the corresponding author on reasonable request, subject to institutional and ethical considerations.

References

1. Campbell E, Eddy E, Isabel X, Bateman S, Gosselin B, Côté-Allard U, Scheme E. Screen Guided Training Does Not Capture Goal-Oriented Behaviours: Learning Myoelectric Control Mappings From Scratch Using Context Informed Incremental Learning. IEEE Trans Neural Syst Rehabil Eng. 2025;33:332–42. https://doi.org/10.1109/TNSRE.2024.3518059.
2. Chadwell A, Kenney L, Thies S, Head J, Galpin A, Baker R. Addressing unpredictability may be the key to improving performance with current clinically prescribed myoelectric prostheses. Sci Rep. 2021;11:3300. https://doi.org/10.1038/s41598-021-82764-6.

3. Farina D, Merletti R, Enoka RM. The extraction of neural strategies from the surface EMG: 2004–2024. J Appl Physiol (1985). 2025;138(1):121–35. https://doi.org/10.1152/japplphysiol.00453.2024.
4. Farrell TR, Weir RFF. The optimal controller delay for myoelectric prostheses. IEEE Trans Neural Syst Rehabil Eng. 2007;15(1):111–8. https://doi.org/10.1109/TNSRE.2007.891391.
5. Freitas MLB, Mendes Junior JJA, La Banca WF, Stevan SL Jr. Study of the relevance of gender in the classification of hand gestures by electromyography-based recognition systems. Res Biomed Eng. 2021;37:361–73. https://doi.org/10.1007/s42600-021-00145-4.
6. Heerschop A, van der Sluis CK, Bongers RM. Training prosthesis users to switch between modes of a multi-articulating prosthetic hand. Disabil Rehabil. 2024;46(1):187–98. https://doi.org/10.1080/09638288.2022.2157055.
7. Mamidanna P, Gholinezhad S, Farina D, Dideriksen JL, Dosen S. Measuring and monitoring skill learning in closed-loop myoelectric hand prostheses using speed-accuracy tradeoffs. J Neural Eng. 2024;21(2):026008. https://doi.org/10.1088/1741-2552/ad2e1c.
8. Mendes Junior JJA, Campos DP, Dias TS, Siqueira HV, Stevan SL Jr, Pichorim SF. Independent component analysis in multi-channel forearm surface electromyography processing on armband approach for hand gesture classification. Res Biomed Eng. 2020;36:439–48. https://doi.org/10.1007/s42600-020-00082-8.
9. Radmand A, Scheme E, Englehart K. A characterization of the effect of limb position on EMG features to guide the development of effective prosthetic control schemes. Annu Int Conf IEEE Eng Med Biol Soc. 2014;2014:662–7. https://doi.org/10.1109/EMBC.2014.6943678.
10. Reaz MBI, Hussain MS, Mohd-Yasin F. Techniques of EMG signal analysis: detection, processing, classification and applications. Biol Proced Online. 2006;8:11–35. https://doi.org/10.1251/bpo115.
11. Reis GL. Controle de um manipulador robótico utilizando sensores inerciais e eletromiografia [master's dissertation]. São João del-Rei, Brazil: Universidade Federal de São João del-Rei / CEFET-MG; 2014.
12. Santos TMO, Barroso MFS, Ricco RA, Nepomuceno EG, Alvarenga ELFC, Penoni ACO, Santos AF. A low-cost wireless system of inertial sensors to postural analysis during human movement. Measurement. 2019;148:106933. https://doi.org/10.1016/j.measurement.2019.106933.
13. Santos TMO, Ricco RA, Barroso MFS. Applied sensor fusion: tuning parameters of CF and KF by means of evolution strategies. IEEE Lat Am Trans. 2020;18(7):1272–9. https://doi.org/10.1109/TLA.2020.9099769.
14. Simon AM, Newkirk K, Miller LA, Turner KL, Brenner K, Stephens M, Hargrove LJ. Implications of EMG channel count: enhancing pattern recognition online prosthetic testing. Front Rehabil Sci. 2024;5:1345364. https://doi.org/10.3389/fresc.2024.1345364.
15. Tosin MC, Cene VH, Balbinot A. Statistical feature and channel selection for upper limb classification using sEMG signal processing. Res Biomed Eng. 2020;36:411–27. https://doi.org/10.1007/s42600-020-00080-w.

16. Wang B, Li J, Hargrove L, Kamavuako EN. Unravelling influence factors in pattern recognition myoelectric control systems: the impact of limb positions and electrode shifts. Sensors. 2024;24(15):4840. https://doi.org/10.3390/s24154840.
17. Won J, Iwase M. Highly responsive robotic prosthetic hand control considering electrodynamic delay. Sensors. 2025;25(1):113. https://doi.org/10.3390/s25010113.
18. Wu H, Dyson M, Nazarpour K. Arduino-based myoelectric control: towards longitudinal study of prosthesis use. Sensors. 2021;21(3):763. https://doi.org/10.3390/s21030763.

Figures



Figure 1

Original experimental platform and sensor placement. (A) Inertial module mounted on the distal forearm to estimate proximal arm orientation. (B) Bipolar forearm electrodes used for single-channel sEMG acquisition, with a separate reference electrode. (C) LEGO robotic manipulator used as a rapid-prototyping and visual-feedback platform. The robot reproduced yaw, pitch, and effector opening/closing; it was not the intended final target device. Photographs are from the authors' original 2014 research archive (Reis 2014)

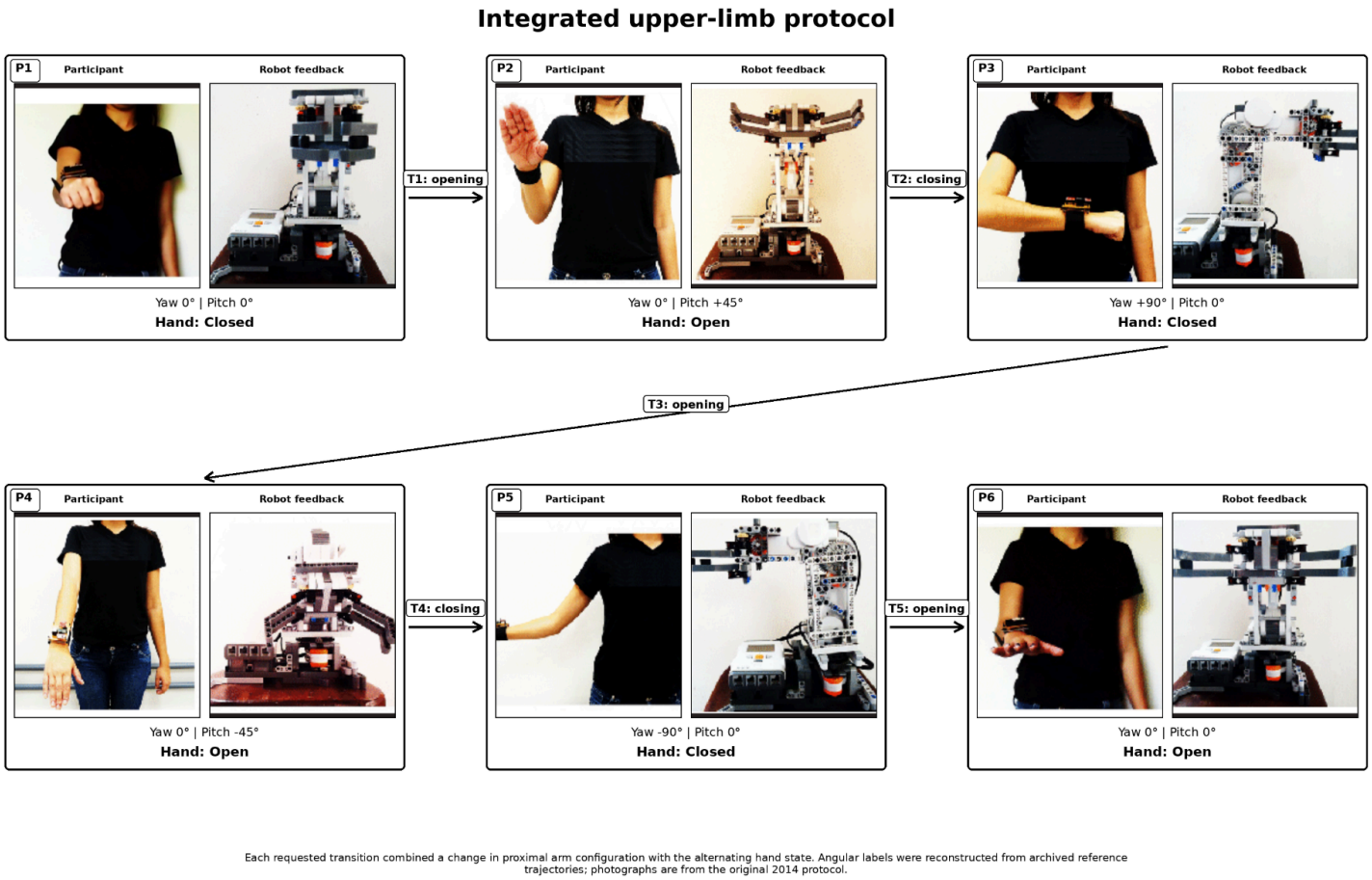


Figure 2

Integrated upper-limb protocol used in the reanalysis. P1-P6 show the six successive participant configurations together with the corresponding robotic feedback. The reconstructed reference sequence was yaw/pitch 0/0 degrees -> 0/+45 degrees -> +90/0 degrees -> 0/-45 degrees -> -90/0 degrees -> 0/0 degrees. Hand state alternated closed -> open -> closed -> open -> closed -> open, producing T1 opening, T2 closing, T3 opening, T4 closing, and T5 opening. Requested transitions occurred at approximately 10-s intervals during each 60-s trial; each participant completed five repetitions. Photographs are from the authors' original 2014 research archive (Reis 2014)

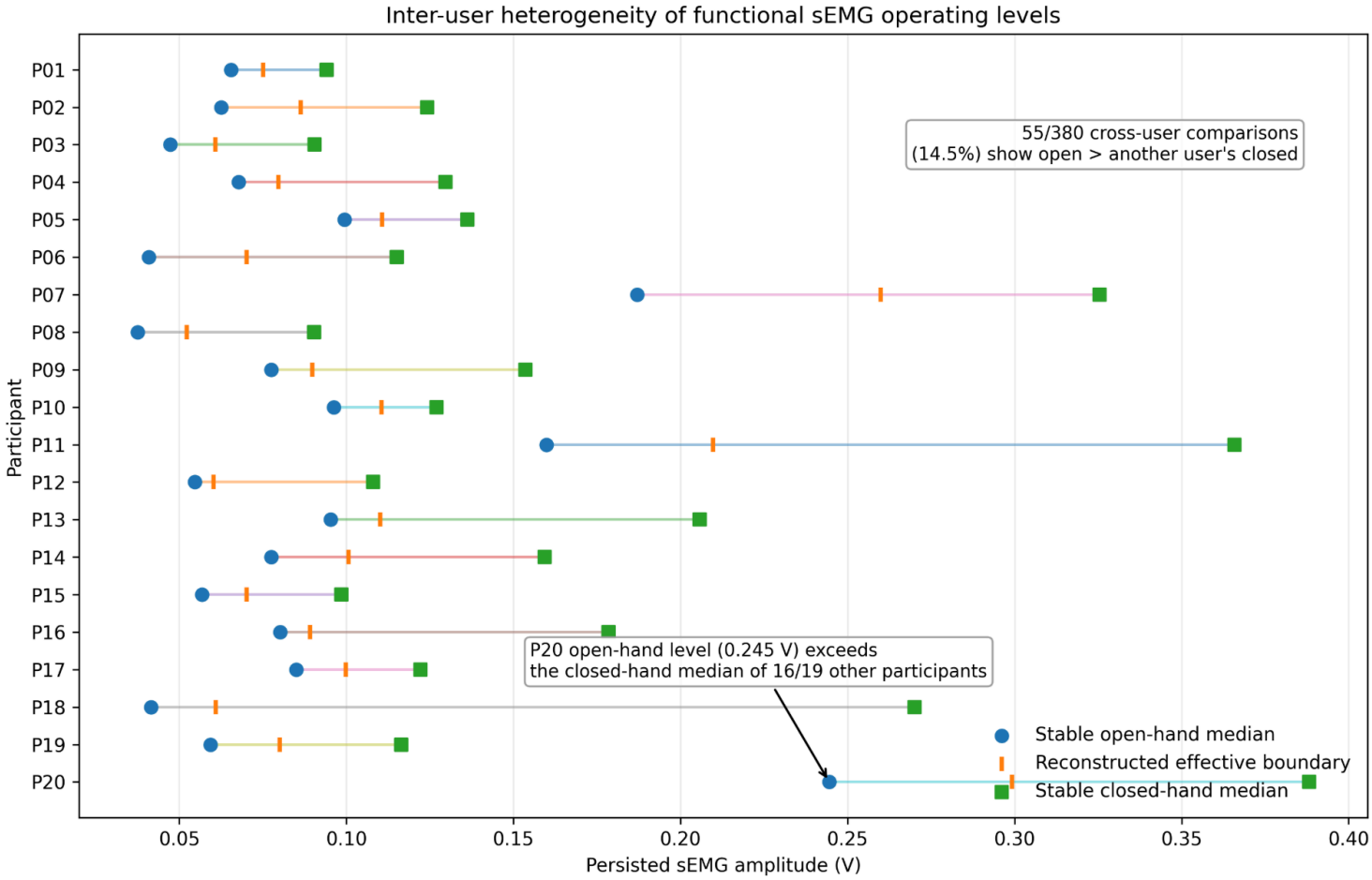


Figure 3

Participant-specific stable sEMG operating levels and reconstructed effective persisted-data boundaries in the hand-only condition. Circles indicate the participant median for the stable open-hand state, triangles the stable closed-hand state, and crosses the reconstructed effective boundary. The vertical segments emphasize within-participant separation, whereas the displacement of entire ranges across P01-P20 emphasizes between-user heterogeneity. The annotation for P20 illustrates that an open-hand value for one user can exceed the closed-hand value of many others. Boundaries are retrospective descriptions of the persisted decision logic and are not the exact original online calibration constants

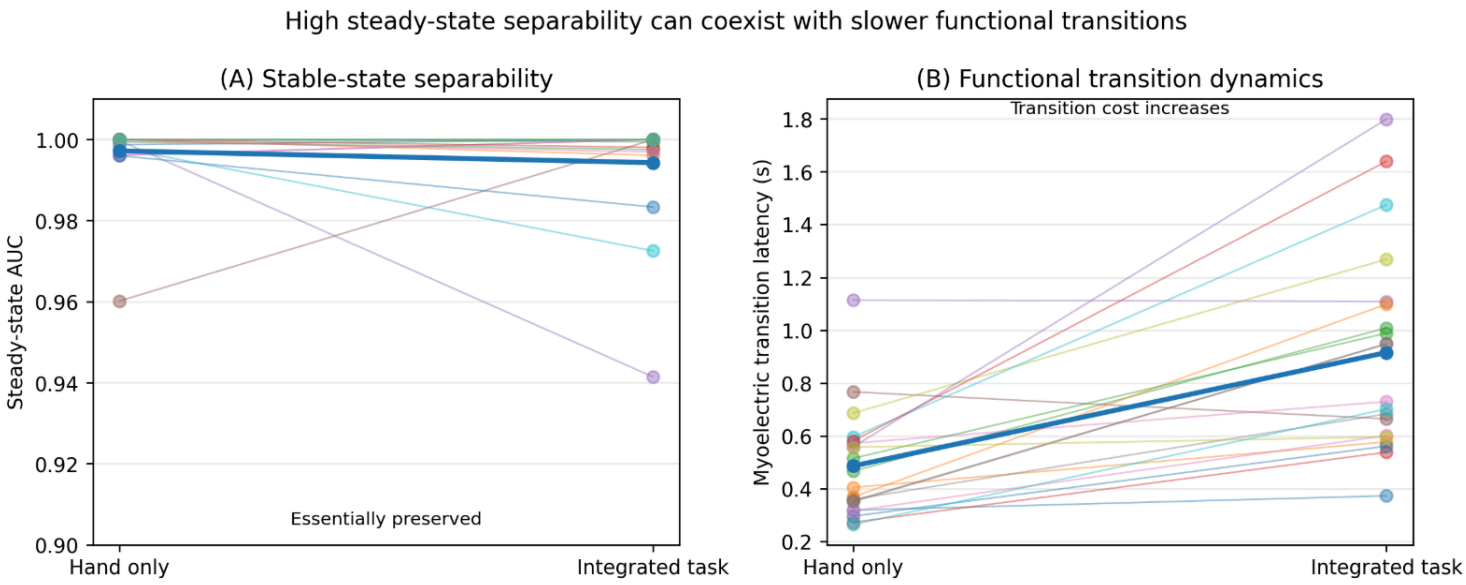


Figure 4

Dissociation between sustained-state discrimination and transition timing. (A) Participant-level stable-state AUC in hand-only and integrated tasks. Values near 1 indicate that, once established, open and closed hand states remained highly distinguishable. (B) Participant-level myoelectric transition midpoint (t50). In contrast to AUC, transition time increased substantially in the integrated condition. Thin lines represent participants; the overlaid summary emphasizes the paired condition change

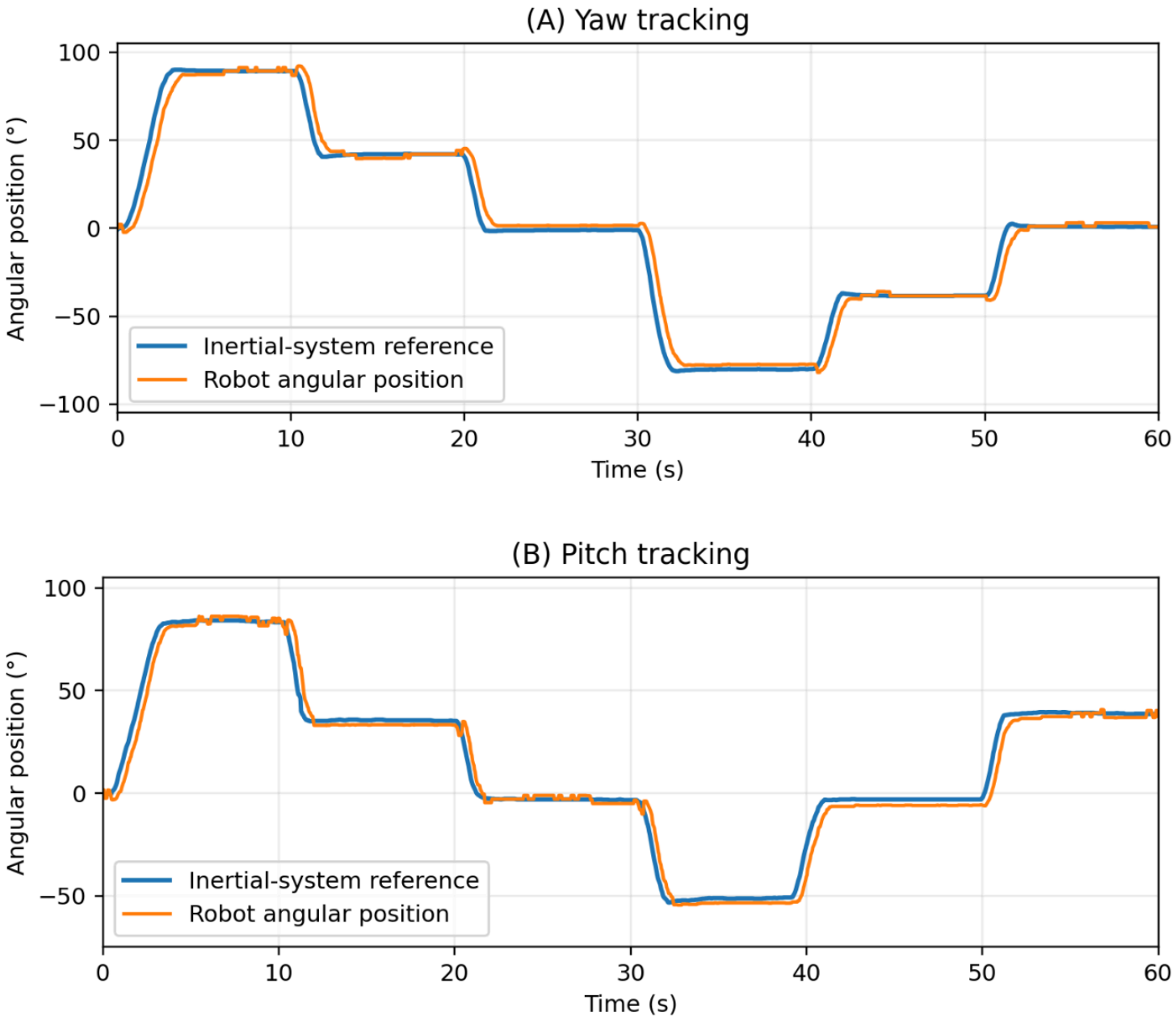


Figure 5

Representative platform-level tracking validation from the original system. (A) Yaw and (B) pitch: the robotic joint position follows the inertial-system reference across step-like 60-s validation trajectories. The original study reported low settling time, no sustained oscillation around commanded positions, and angular tracking error below 1 degree (Reis 2014). The curves were redrawn from the original dissertation plots for visual consistency; no numerical result in the present secondary analysis was derived from the redrawn traces. These validation trajectories document the feedback platform and are distinct from the participant-level integrated trials analysed in Figures 6 and 7

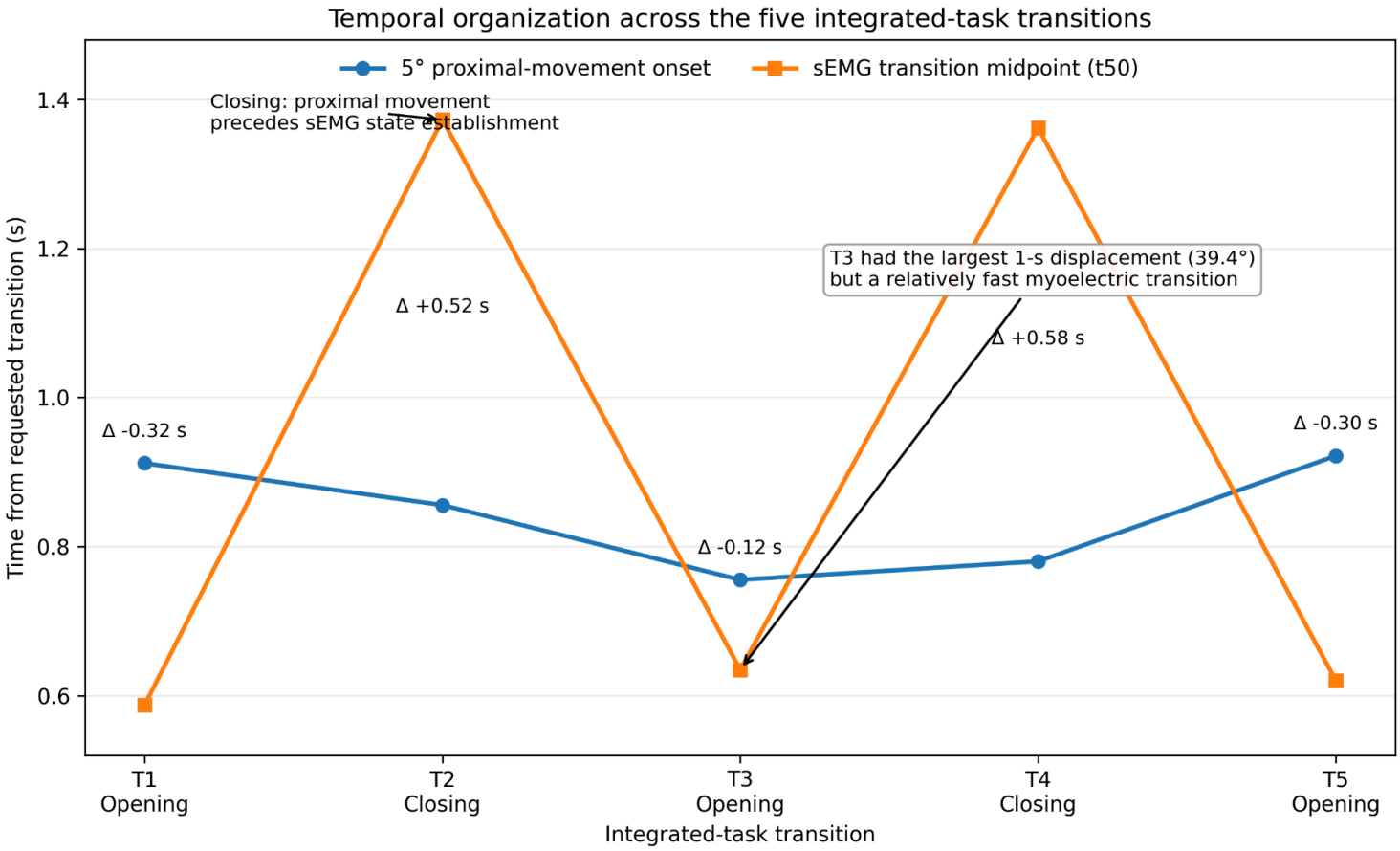


Figure 6

Event-centred temporal tracking and organization of the five transitions in the integrated task. Lines show mean time from the requested transition to the 5-degree proximal-movement onset and to the normalized sEMG midpoint (t50). Delta labels indicate sEMG t50 minus proximal onset: negative values mean the myoelectric midpoint preceded the 5-degree movement criterion; positive values mean proximal movement was already underway. T3 had the largest first-second displacement but a relatively short t50, arguing against a simple movement-magnitude explanation. Opening/closing comparisons remain confounded by the fixed event sequence

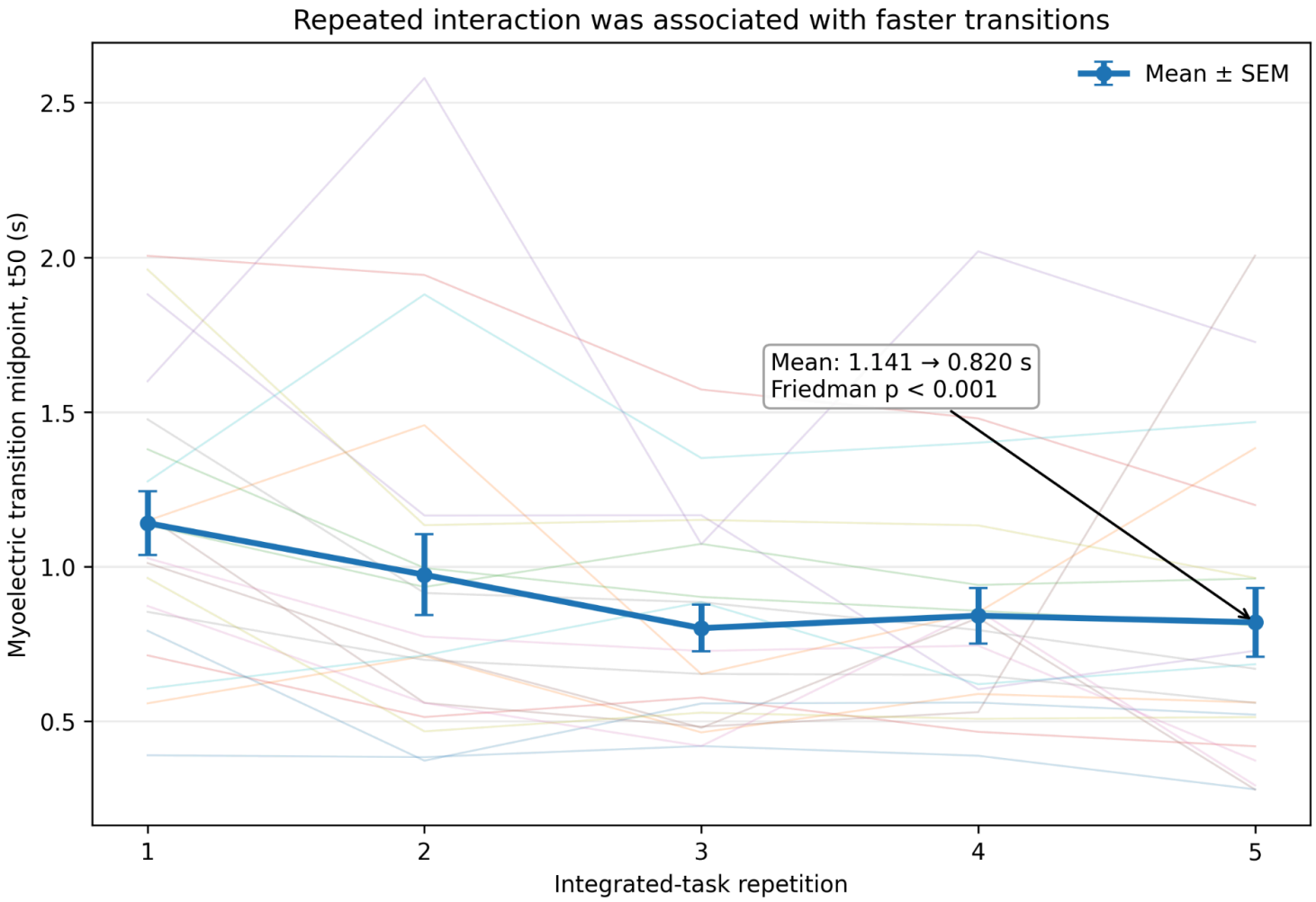


Figure 7

Myoelectric transition midpoint (t50) across the five repetitions of the integrated task. Light lines show participant trajectories and the bold line shows the group mean. Mean t50 decreased from 1.141 s in repetition 1 to 0.820 s in repetition 5 (Friedman $p<0.001$). The pattern is interpreted as task familiarization/adaptation; fatigue and subjective workload were not directly measured